Calix[4]arenes as Selective Extracting Agents. An NMR Dynamic and Conformational Investigation of the Lanthanide(III) and Thorium(IV) Complexes

Bernard Lambert,[†] Vincent Jacques,[†] Alexander Shivanyuk,[‡] Susan E. Matthews,[‡] Abdi Tunayar,[‡] Marc Baaden,[§] Georges Wipff,[§] Volker Böhmer,[‡] and Jean F. Desreux*,[†]

Coordination and Radiochemistry, University of Liège, Sart Tilman (B6), B-4000 Liège, Belgium, and Institut für Organische Chemie, Johannes-Gutenberg-Universität, D-55099, Mainz, Germany, and Laboratoire MSM, UMR 7551 CNRS, Institut de Chimie, 4, rue B. Pascal, 67000 Strasbourg, France

Received June 15, 1999

The lanthanide and Th^{4+} complexes with calix[4]arene ligands substituted either on the narrow or at the wide rim by four coordinating groups behave totally differently as shown by an NMR investigation of the dia- and paramagnetic complexes. Solutions of complexes were prepared by reacting anhydrous metal perchlorate salts with the ligands in dry acetonitrile (CAUTION). Relaxation time T_1 titrations of acetonitrile solutions of Gd^{3+} by calixarenes indicate that ligands substituted on the narrow rim form stable 1:1 complexes whether they feature four amide groups (**1**) or four phosphine oxide functions. In contrast, a ligand substituted by four (carbamoylmethyl)-diphenylphosphine oxide moieties on the wide rim (**3**) and its derivatives form polymeric species even at a 1:1 ligand/metal concentration ratio. Nuclear magnetic relaxation dispersion (NMRD) curves (relaxation rates $1/T_1$ vs magnetic field strength) of Gd^{3+}, Gd^{3+}•**1** and Gd^{3+}•**3** perchlorates in acetonitrile are analyzed by an extended version of the Solomon−Bloembergen−Morgan equations. A comparison of the calculated rotational correlation times τ_r shows that ligand **3** forms oligomeric Gd^{3+} species. The chelates of ligand **1** are axially symmetric (C_4 symmetry), and the paramagnetic shifts induced by the Yb^{3+} ion are accounted for quantitatively. The addition of water or of nitrate ions does not modify the geometry of the complex. The metal chelates of **3** and its derivatives adopt a C_2 symmetry, and the paramagnetic shifts are interpreted on a semiquantitative basis only. Water and NO_3^- ions completely labilize the complexes of the heavy lanthanides. The very high selectivity of ligand **3** through the lanthanide series stems from a complex interplay of factors.

Introduction

The processing of nuclear waste before disposal relies most often on solvent extraction procedures, and a large number of extracting agents have been synthesized and tested with the aim of separating metal ions more effectively. However, despite years of efforts, an efficient separation of Am^{3+} from Eu^{3+} in strongly acidic media remains an elusive goal, and several research groups have recently suggested entirely new approaches to solve this problem.[1] The extraction properties and the selectivity of calixarene derivatives have been evaluated recently for this purpose.[2] The calix moiety is easily substituted by a wide variety of coordinating groups, and its size and steric requirements can be modified nearly at will[3] to allow inter- and/or intragroup separations of metal ions. Of particular interest is a calix[4]arene bearing CMPO-like groups that proved[4] to be a remarkably selective extracting agent of the lanthanides (CMPO = (*N*,*N*-diisobutylcarbamoyl)octylphenylphosphine oxide). Elucidating the origin of this selectivity is a difficult task because the efficiency of an extraction process depends on a number of factors, the relative influence of which is difficult to assess on the basis of extraction data alone. Indeed, slope analyses of distribution curves or organic phase saturation experiments yield only the approximate overall composition of the extracted species. In the present study, NMR spectroscopy is applied to an analysis of the complexation of trivalent lanthanides and Th^{4+} by calix[4]arenes **1**−**8** (Chart 1). Ligands **1** and **2** are substituted by four identical groups on the narrow opening (or lower rim) of the calix unit, while ligands **3**−**8** feature two or four coordinating moieties on the wide opening (or upper rim). The extraction behaviors of all these ligands have been reported[2,4] or are under investigation.

The present NMR analysis starts with the simplest systems, that is, an anhydrous metal perchlorate salt in dry acetonitrile to which increasing quantities of a ligand are added to form complexes. Nuclear magnetic relaxation and NMR spectroscopy studies of dia- and paramagnetic complexes are carried out on these mixtures to obtain quantitative dynamic and structural information. Water and coordinating anions are then added in order to study competing effects and to move closer to practical conditions. Of particular relevance are two NMR techniques that proved to be fruitful in the study of paramagnetic lanthanide chelates. The first technique is often called relaxivity and is based on the measurement of the longitudinal relaxation times T_1 of the solvent peak of solutions of Gd^{3+} complexes at different frequencies (or field strength), yielding nuclear mag-

[†] University of Liège.
[‡] Johannes-Gutenberg-Universität.
[§] Institut de Chimie.

(1) (a) Zhu, Y.; Chen, J.; Jiao, R. *Solvent Extr. Ion Exch.* **1996**, *14*, 61−68. (b) Kolarik, Z.; Müllich, U.; Gassner, F. *Solvent Extr. Ion Exch.* **1999**, *17*, 23−32.
(2) Arnaud-Neu, F.; Böhmer, V.; Dozol, J.-F.; Grüttner, C.; Jakobi, R. A.; Kraft, D.; Mauprivez, O.; Rouquette, H.; Schwing-Weill, M.-J.; Simon, N.; Vogt, W. *J. Chem. Soc., Perkin Trans. 2* **1996**, 1175−1182.
(3) Böhmer, V. *Angew. Chem., Int. Ed. Engl.* **1995**, *34*, 713−745.
(4) Delmau, L. H.; Simon, N.; Schwing-Weill, M.-J.; Arnaud-Neu, F.; Dozol, J.-F.; Eymard, S.; Tournois, B.; Böhmer, V.; Grüttner, C.; Musigmann, C.; Tunayar, A. *J. Chem. Soc., Chem. Commun.* **1998**, 1627−1628.

10.1021/ic990683n CCC: $19.00
Published on Web 04/19/2000

Chart 1

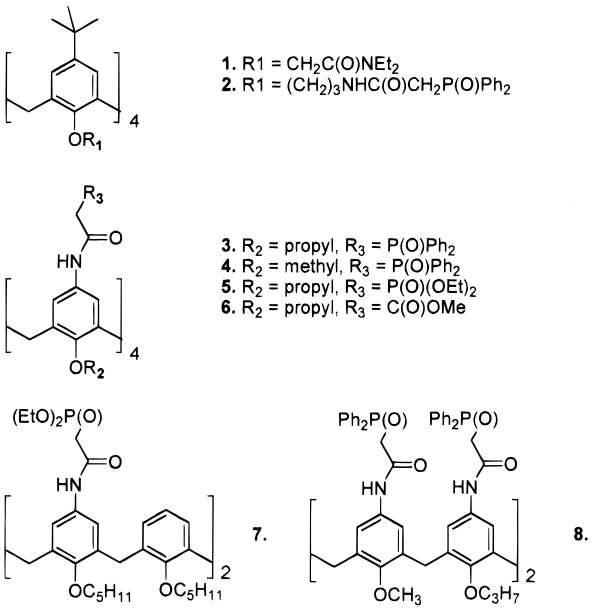

netic relaxation dispersion (NMRD) curves. This approach allows one to investigate the dynamic behavior of Gd^{3+}-containing species, and it has been extensively applied to the study of aqueous solutions of highly stable chelates useful as contrast agents for magnetic resonance imaging.[5,6] However, to our knowledge, NMRD curves have not yet been reported for nonaqueous Gd^{3+} solutions. The second technique takes advantage of the large chemical shifts induced by the paramagnetic lanthanide ions, most often Yb^{3+}. These shifts are essentially of dipolar origin and are directly related to the conformation of the metal complexes.[5] Most often, the high lability of the lanthanide complexes precludes quantitative structural analyses, and reliable conformational studies are feasible only if a ligand forms highly stable and rigid chelates. These conditions are met for only a limited number of lanthanide derivatives,[7] but it will be shown here that calix[4]arene complexes lend themselves to a quantitative NMR spectroscopic analysis even if the solution behavior of some of these compounds is not as simple as anticipated, a phenomenon that leads to uncertainties.

Experimental Section

Anhydrous lanthanide chlorides were purchased from Strem. Anhydrous $Th(ClO_4)_4$ and lanthanide perchlorates, $Ln(ClO_4)_3$ with Ln = La, Gd, Eu, Yb, Lu, were prepared by a slight modification of the procedure reported by Pascal et al.[8] As described by these authors, chlorine trioxide dimer Cl_2O_6 was prepared by ozonolysis of ClO_2 and was distilled directly into a reactor containing a hydrated metal perchlorate salt at −78 °C. The anhydrous salt was obtained upon raising the temperature to 80 °C under vacuum until a constant weight was reached. The metal content of the final product was determined by complexometry with a potentiometric end point detection.[9] CAUTION: lanthanide perchlorates are known to be potential explosives when brought into contact with organic materials. It is advisable to use only small amounts of a metal salt at a time with proper care and in a glovebox.

All manipulations were carried out under argon in a Jacomex (Livry-Gargan, France) glovebox equipped with an atmosphere purification system ensuring that the water and oxygen levels remained below 0.5 and 5 ppm, respectively. An Ohaus AP250D balance (Florham Park, NJ) with a precision of 0.02 mg was placed in the glovebox and used for weighing samples of ligands and metal salts. The water content of the solutions was measured with a Tacussel Aquaprocessor (Radiometer Analytical, Lyon, France). In the worst cases, the water/lanthanide ratios were well below 0.1. Calix[4]arenes **1** and **2**−**8** were synthesized as reported by Arduini et al.[10] and by Böhmer et al.[2,11−13] Solutions of the metal complexes suitable for NMR studies were prepared by dissolving in acetonitrile known quantities of an anhydrous metal salt and of a ligand previously dried under vacuum. Typically, a solution of a 50% excess of $Yb(ClO_4)_3$ (6.54 mg, 0.0138 mmol) in 0.25 mL of dried deuterated acetonitrile was added to 15 mg (0.0092 mmol) of ligand **3** suspended in 0.25 mL of the same solvent. All ligands dissolved immediately upon addition of the metal salts, and no changes in the NMR spectra of the complexes were observed over periods of several months provided the solutions were kept in tightly closed vessels in a glovebox.

The NMR spectra were recorded on a Avance DRX-400 spectrometer (Bruker) equipped with a temperature controller (±0.1 K). The COSY 2D spectra were typically recorded with 1024 data points in t_2 and 512 data points in t_1 with a bandwidth of 3−25 kHz. A 0°-shifted sine bell apodization function was applied in both dimensions prior to the Fourier transformation. The exchange spectroscopy (EXSY) experiments were performed using a phase-sensitive pulse sequence with $2048t_2 \times 2048t_1$. Both dimensions were apodized by a 90°-shifted sine bell function without zero-filling. The mixing time t_m was 20 ms for the paramagnetic Yb^{3+} complexes. A 500 ms mixing time was used in the rotating-frame Overhauser enhancement spectroscopy (ROESY) experiments with a 1024×512 data set. Zero-filling was applied to obtain a 1024×1024 size. Exchange and nuclear Overhauser effect (nOe) cross-peaks were distinguished thanks to their sign that was identical or opposite to the sign of the diagonal peaks, respectively. The NMR spectrum of Yb^{3+}•**3** is strongly dependent on temperature and in many instances, several peaks overlap to the point of being indistinguishable even as shoulders. One- and two-dimensional spectra had to be recorded at 5 K intervals between 243 and 345 K before the exact number of peaks and their relative areas could be accurately determined. The 1D ^{31}P spectra with complete proton decoupling were recorded at 162 MHz and referenced to a 85% aqueous H_3PO_4 solution. Longitudinal relaxation times were collected at 20 MHz on a Minispec 120 (Bruker) at 25 °C, and NMR dispersion curves were recorded at the University of Mons-Hainaut, Belgium, on a field-cycling relaxometer described elsewhere.[14,15]

(5) Peters, J. A.; Huskens, J.; Raber, D. J. *Prog. Nucl. Magn. Reson. Spectrosc.* **1996**, *28*, 283−350.
(6) Aime, S.; Botta, M.; Fasano, M.; Terreno, E. *Chem. Soc. Rev.* **1998**, *27*, 19−29.
(7) So far, the dipolar equations have been applied successfully to the lanthanide chelates of pyridine-2,6-dicarboxylic acid, diethylenetriaminepentaacetic acid, various derivatives of 1,4,7,10-tetraazacyclododecane-1,4,7,10-tetraacetic acid, texaphyrins, tris(pyrazolyl)boron and podates. (a) Desreux, J. F.; Reilley, C. N. *J. Am. Chem. Soc.* **1976**, *98*, 2105−2109. (b) Jenkins, B. G.; Lauffer, R. B. *Inorg. Chem.* **1988**, *27*, 4730−4738. (c) Jacques, V.; Desreux, J. F. *Inorg. Chem.* **1994**, *33*, 4048−4053. (d) Forsberg, J. H.; Delaney, R. M.; Zhao, Q.; Harakas, G.; Chandran, R. *Inorg. Chem.* **1995**, *34*, 3705−3715. (e) Desreux, J. F.; Loncin, M. F. *Inorg. Chem.* **1986**, *25*, 69−74. (f) Lisowski, J.; Sessler, J. L.; Lynch, V.; Mody, T. D. *J. Am. Chem. Soc.* **1995**, *117*, 2273−2285. (g) Stainer, M. V. R.; Takats, J. *J. Am. Chem. Soc.* **1983**, *105*, 410−415. (h) Renaud, F.; Piguet, C.; Bernardinelli, G.; Bünzli, J.-C. G.; Hopfgartner, G. *J. Am. Chem. Soc.* **1999**, *121*, 9326−9342.
(8) Favier, F.; Pascal, J. L. *J. Chem. Soc., Dalton Trans.* **1992**, 1997−2002.
(9) Reilley, C. N.; Schmid, R. W.; Lamson, D. W. *Anal. Chem.* **1958**, *30*, 953−957.
(10) Arduini, A.; Ghidini, E.; Pochini, A.; Ungaro, R.; Andreetti, G. D.; Calestani, G.; Ugozzoli, F. *J. Inclusion Phenom.* **1988**, *6*, 119−134.
(11) Barboso, S.; Carrera, A. G.; Matthews, S. E.; Arnaud-Neu, F.; Böhmer, V.; Dozol, J.-F.; Rouquette, H.; Schwing-Weill, M.-J. *J. Chem. Soc., Perkin Trans. 2* **1999**, *2*, 719−723.
(12) Matthews, S. E.; Saadioui, M.; Böhmer, V.; Barboso, S.; Arnaud-Neu, F.; Schwing-Weill, M.-J.; Garcia Carrera, A.; Dozol, J.-F. *J. Prakt. Chem.* **1999**, *341*, 264−273.
(13) Shivanyuk, A.; Tunayar, A.; Böhmer, V. Unpublished results.
(14) Vander Elst, P.; Maton, F.; Laurent, S.; Seghi, F.; Chapelle, F.; Muller, R. N. *Magn. Reson. Med.* **1997**, *38*, 604−614.
(15) Koenig, S. H.; Brown, R. D. *Prog. Nucl. Magn. Reson. Spectrosc.* **1990**, *22*, 487−567.

Molecular mechanics geometry optimizations of the lanthanide complexes of ligand **1** were performed as reported by Cundari et al.[16] with the force field approach used in Chem 3D Plus (Cambridge Scientific Computing, Cambridge, MA). The force field parameters of Hay[17] and Cundari et al.[16] were used throughout. The geometry of the Yb^{3+} complexes of ligand **3** was model-built by molecular dynamics simulations[18] in the gas phase using the Amber 4.1 program. The distance between two opposite methylene groups in the calix unit was constrained to a series of fixed values between 6 and 8 Å, and the remaining system was left free to relax.

Results and Discussion

Preparation of Lanthanide Calix[4]arene Complexes. Well-resolved NMR spectra of the lanthanide complexes with the calix[4]arene tetraamide **1** were readily obtained after mixing stoichiometric amounts of a hydrated or an anhydrous metal perchlorate salt with the ligand in deuterated acetonitrile. On the other hand, following the same procedure with tetra-CMPO ligand **3** led only to NMR spectra featuring poorly shifted broad peaks. Extraction of Yb^{3+} ions with **3** from nitrate or chloride aqueous phases yielded the same results. Working under anhydrous conditions appeared more promising, but insufficiently resolved spectra were obtained if the syntheses were carried out with anhydrous Yb(III) triflate in acetonitrile, and complicated spectra with numerous partially broadened peaks were recorded if the starting material was anhydrous $YbCl_3$ in deuterated methanol. In view of these difficulties, it was decided to prepare anhydrous metal perchlorate salts according to the method proposed by Pascal et al.[8,19] This approach requires the preparation of anhydrous chlorine trioxide, Cl_2O_6, on a vacuum line as well as the handling of all compounds in a high-quality glovebox under an inert atmosphere. Despite these difficulties, Pascal's method was deemed more appropriate than other techniques[20,21] that are thwarted by the partial decomposition of the solvent[22] or by liberation of methanol. Notwithstanding their difficult preparation and their explosive characteristics (CAUTION: see experimental part), anhydrous lanthanide perchlorates are attractive starting materials for NMR studies because they allow an analysis of simple systems: metal ions with very poorly coordinating anions in an organic solvent in the absence of water.

Relaxivity Measurements and Solution Behavior of the Gd^{3+} Calix[4]arene Complexes. The difficulties encountered when attempting to record well-resolved NMR spectra (vide infra) were tentatively assigned to the formation of oligomeric metal calixarene species. It was thus decided to measure the longitudinal relaxation rate $1/T_1$ of the solvent NMR peak of anhydrous acetonitrile solutions of the Gd^{3+} complexes with ligands **1**−**4** and **6**−**7**. During the past few years, numerous relaxation studies have been carried out on aqueous solutions of highly stable polyaminopolyacetic Gd^{3+} chelates. It was shown[5,23] that plots of the relaxation rate of the solvent peak per millimole of Gd^{3+} (relaxivity, in s^{-1} mM^{-1}) vs the Larmor frequency (or magnetic field strength), also called NMRD curves, give insight into the formation and the dynamic behavior of the Gd^{3+} complexes. The relaxation rate $1/T_{1is}$ of solvent molecules in the inner coordination sphere of a Gd^{3+} ion is well accounted for by the Solomon−Bloembergen−Morgan equations:

$$\frac{1}{T_{1is}} = \frac{P_M q_{solvent}}{[solvent]} \frac{1}{(T_{1M} + \tau_m)} \quad (1)$$

$$\frac{1}{T_{1M(dip)}} = \frac{2}{15}\left(\frac{\mu_0}{4\pi}\right)^2 \frac{\gamma_I^2 \mu_B^2 g_e^2 S(S+1)}{r^6}\left[\frac{3\tau_c}{1+\omega_I^2\tau_c^2} + \frac{7\tau_c}{1+\omega_S^2\tau_c^2}\right] \quad (2)$$

According to eqs 1 and 2, $1/T_{1is}$ depends on $q_{solvent}$, the number of solvent molecules directly coordinated to the metal ion, on P_M, the molar fraction of the metal, on r, the distance between Gd^{3+} and the solvent protons, and on the correlation time τ_c. In these equations, ω_S and ω_I are the Larmor frequencies of the electron and of the proton, and the other factors have their usual meaning. The correlation time τ_c is given by

$$\frac{1}{\tau_c} = \frac{1}{\tau_S} + \frac{1}{\tau_m} + \frac{1}{\tau_r} \quad (3)$$

where τ_c depends on the smallest of three correlation times, τ_r, the mean rotational correlation time of the Gd^{3+} species, τ_s, the metal electronic relaxation time, or τ_m, the mean residence time of the solvent molecules in the first coordination sphere of the metal ion. The frequency dependence of τ_S is accounted for by the equation

$$\frac{1}{\tau_s} = \frac{1}{5\tau_{s0}}\left[\frac{\tau_v}{1+\omega_s^2\tau_v^2} + \frac{4\tau_v}{1+4\omega_s^2\tau_v^2}\right] \quad (3)$$

where τ_{s0} and τ_v are the electronic relaxation time at zero field and the correlation time for the modulation of the zero-field splitting, respectively. Outer-sphere effects are accounted for by the Freed equations.[23] The complexation of Gd^{3+} by a ligand reduces the solvation of the metal ion and leads to a decreased relaxivity because solvent molecules relax more slowly in the bulk of the solution than in the immediate surroundings of the metal ions. Moreover, rapidly rotating small Gd^{3+} chelates with small τ_r values display S-shaped curves with an inflection point between 1 and 10 MHz. By contrast, a relaxivity maximum at about 20 MHz is observed for slowly tumbling species because the rotational correlation time is no longer the major contributor to relaxivity. It is the frequency dependence of the electronic relaxation time τ_S that brings about relaxivity maxima as reported for Gd^{3+} complexes of high molecular weight ligands.[5,23] Numerous NMRD curves have recently been reported for Gd^{3+}-containing MRI contrast agents, and the complicated interplay between the correlation times has been investigated in great details.[5−6,23,24] All these studies were carried out in water, but it will be shown here that relaxivity measurements in organic solvents are also susceptible to yield interesting information on the solution behavior of lanthanide chelates.

Figure 1 presents a plot of the relaxivity of anhydrous degassed acetonitrile solutions of mixtures of Gd^{3+} perchlorate with different calix[4]arenes vs the ligand/metal concentration ratio at 25 °C and 20 MHz. As expected, the relaxivity of a Gd^{3+} solution linearly decreases when ligand **1** is added until a

(16) Cundari, T. R.; Moody, E. W.; Sommerer, S. O. *Inorg. Chem.* **1995**, *34*, 5989−5999.
(17) Hay, B. P. *Inorg. Chem.* **1991**, *30*, 2876−2884.
(18) Baaden, M.; Troxler, L.; Wipff, G.; Böhmer, G. *Supramol. Chem.*, in press.
(19) Pascal, J. L.; Potier, J.; Zhang, C. S. *J. Chem. Soc., Dalton Trans.* **1985**, 297−305.
(20) Gansow, O. A.; Triplett, K. B. U.S. Patent, 4,257,955, 1981; pp 1−8.
(21) Desreux, J. F.; Renard, A.; Duyckaerts, G. *J. Inorg. Nucl. Chem.* **1977**, *39*, 1587−1591.
(22) Ciampolini, M.; Fabbrizzi, L.; Perotti, A.; Poggi, A.; Seghi, B.; Zanobini, F. *Inorg. Chem.* **1987**, *26*, 3527−3533.
(23) Caravan, P.; Ellison, J. J.; McMurry, T. J.; Lauffer, R. B. *Chem. Rev.* **1999**, *99*, 2293−2352.

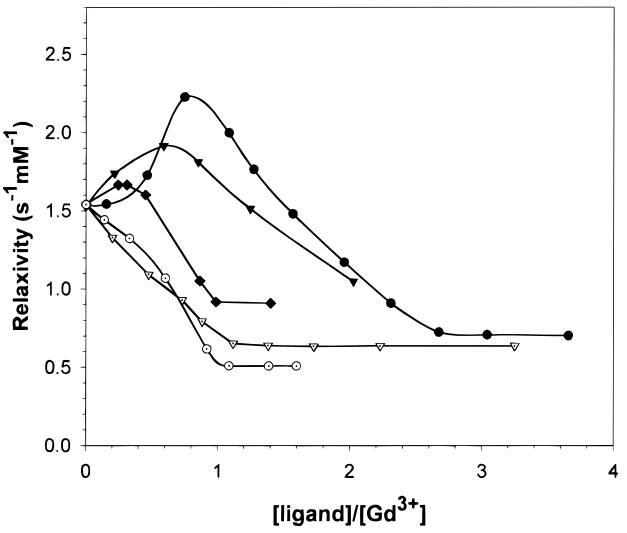

Figure 1. Plot of the observed longitudinal relaxation rates $1/T_1$ per mM of Gd^{3+} (relaxivity in s^{-1} mM^{-1}) of anhydrous acetonitrile solutions vs the ligand/Gd^{3+} concentration ratio for ligands **1** (▽), **2** (⊙), **3** (●), **4** (▼), and **6** (◆) at 298 K and 20 MHz. All solutions are approximately 1 mM in metal ion.

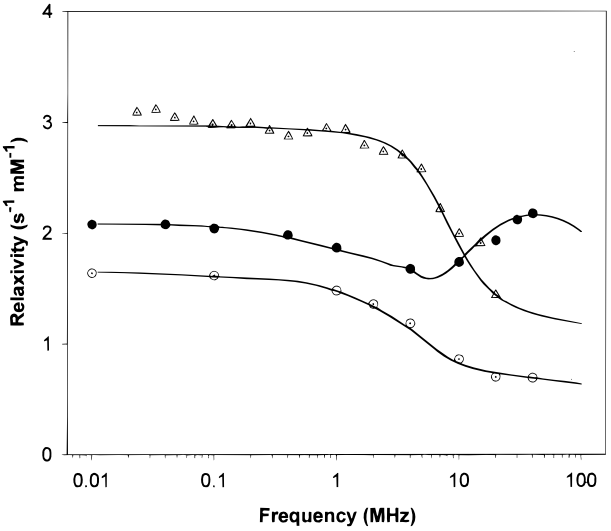

Figure 2. NMR dispersion curves of anhydrous acetonitrile solutions of uncomplexed Gd^{3+} (△) and 1:1 mixtures of Gd^{3+} with ligands **1** (⊙) and **3** (●) at 298 K. All solutions are approximately 1 mM in metal ion. The solid lines were computed by the computer program developed by Bertini et al.[25]

plateau is reached for a 1:1 concentration ratio. Solvent molecules are thus progressively removed from the first coordination sphere of the metal ion until a highly stable Gd^{3+} complex with **1** is fully formed. Ligand **2** behaves similarly, although the decrease in relaxivity is not strictly linear. Calix[4]arenes **1** and **2** are both substituted on the narrow rim, but their coordinating groups are either very close to the polyaromatic unit or removed by several bonds. This difference has little influence on the relaxivity titration curves that have the shape expected for single stable 1:1 metal complex. By contrast, ligand **3** features an unusual titration curve. The relaxivity first increases until a maximum is reached for a ligand/Gd^{3+} ratio of about 0.8−1. It then slowly decreases until a plateau appears for ratios higher than 2.5. NMR studies clearly indicate that ligand **3** is able to encapsulate lanthanide ions (vide infra), and solvent molecules are thus replaced by coordinating groups just as in the case of **1** and **2**. The relaxivity maximum is assigned to the formation of oligomers that are tumbling sufficiently slowly so that the longer relaxation times of solvent molecules released to the bulk of the solution are more than compensated for by the shorter relaxation times of solvent molecules coordinated to aggregates. This oligomerization does not depend on the length of the alkyl chains that substitute the ligand narrow rim, since a similar relaxation behavior is noted for ligand **4**. Ligands **1** and **2** and **3** and **4** differ by the location of their coordinating arms that are substituting either the narrow or the wide rim of the calix unit. The oligomerization could then be ascribed to the greater flexibility of the ligating functions on the wide rim. This flexibility appears to be a common feature of all ligands substituted on the wide rim because relaxivity maxima are also observed in the titration curves of ligands **6** and **7**. For the former, the carboxamide ester function seems more strongly coordinating than the CMPO group as the relaxivity maximum is followed by a plateau at a 1:1 metal/ligand ratio. For the latter, a small relaxivity maximum is observed at approximately a 1.2 ratio despite the presence of two coordinating groups only (see Supporting Information, Figure S2).

The NMR dispersion curves of anhydrous acetonitrile solutions of uncomplexed Gd^{3+} and of 1:1 mixtures of Gd^{3+} with ligands **1** and **3** are reported in Figure 2. These calixarenes were selected among the ones synthesized for the present study because the NMR spectra of their Yb^{3+} complexes are relatively simple (vide infra). Relaxivity and spectroscopic data can thus be fruitfully combined for these ligands. The NMRD curve of uncomplexed Gd^{3+} has the usual S shape predicted by eqs 1−4 for rapidly rotating small species. As expected, relaxivities of uncomplexed Gd^{3+} solutions are lower in acetonitrile than in water because of the longer distance r between the metal ion and the acetonitrile protons. A quantitative analysis of the NMRD data was performed with a recent version of a computer program that takes into account the splitting D of the S manifold as reported by Bertini and Luchinat.[25] A coordination number of 8 was assumed, and a $Gd^{3+}\cdots N{\equiv}C-CH_3$ distance of 5.3 Å was used in the calculations. Indeed, Fourier transform infrared studies have shown that only one perchlorate anion remains coordinated to lanthanide ions in 0.05 M solutions in anhydrous acetonitrile.[26] This anion was found to be essentially monodentate, and a solvation number of 8 seems reasonable. Moreover, the outer-sphere effect was estimated by Freed's equation[23] assuming a distance of closest approach of 10.5 Å and using the reported[27] diffusion coefficient of acetonitrile. Finally, the residence time τ_m of acetonitrile coordinated to Gd^{3+} was set to the only value that seems to be available in the literature[28] ($\tau_m = 3000$ ps). The best agreement between the calculated and the experimental data collected for uncomplexed Gd^{3+} was obtained with the parameters $\tau_r = 51$ ps, $\tau_{S0} = 64$ ps, $\tau_v = 5$ ps, and $D = 0.016$ cm^{-1}. The Gd^{3+}•**1** chelate also features a simple S-shaped NMRD curve as expected for a rapidly tumbling monomeric species and in full agreement with the titration curve reported in Figure 1. Moreover, the relaxivity of this complex is lower than that of free Gd^{3+} because solvent molecules are removed from the first coordination sphere upon complexation. The quantitative interpretation of the NMRD

(24) Powell, D. H.; Ni Dhubhghaill, O. N.; Pubanz, D.; Helm, L.; Lebedev, Y. S.; Schlaepfer, W.; Merbach, A. E. *J. Am. Chem. Soc.* **1996**, *118*, 9333−9346.
(25) Bertini, I.; Galas, O.; Luchinat, C.; Parigi, G. *J. Magn. Reson.* **1995**, *113*, 151−158.
(26) Bunzli, J. C. G.; Mabillard, C. *Inorg. Chem.* **1986**, *25*, 2750−2754.
(27) Holz, M.; Weingärtner, H. *J. Magn. Reson.* **1991**, *92*, 115−125.
(28) Veselov, I. A.; Shtyrlin, V. G.; Zakharov, A. V. *Koord. Khim.* **1989**, *15*, 567−571.

curve of Gd^{3+}·**1** was performed assuming that only one acetonitrile molecule is directly coordinated to the metal ion in Gd^{3+}·**1**, in keeping with the conformational studies reported below and with a preliminary crystallographic analysis. The best-fit treatment of the NMRD curve of the Gd^{3+}·**1** complex yielded the values $\tau_r = 193$ ps, $\tau_{s0} = 278$ ps, $\tau_v = 2$ ps, and $D = 0.06$ cm^{-1}. Gd^{3+}·**3** exhibits an NMRD curve that is clearly indicative of the formation of oligomers.[6,23] Ligands **1** and **3** have similar molecular sizes, and the τ_r values of their Gd^{3+} complexes should thus be comparable. Because the relaxivity at 30 MHz of Gd^{3+}·**3** is sizeably higher than that of Gd^{3+}·**1** and even than that of free Gd^{3+}, one is led to assume that the CMPO substituents on the wide opening of **3** are sufficiently flexible to form oligomeric structures in which metal ions are coordinated to several calixarene molecules. This hypothesis is in agreement with the interpretation of the relaxivity titration curves presented in Figure 1 and with a recently reported crystallographic analysis of the dimeric structure $Eu_5\mathbf{3}_2(NO_3)_{15}\cdot 2H_2O$ in which one of the metal ions is coordinated to two CMPO arms belonging to different calixarene units.[29] Moreover, small angle neutron scattering studies have shown that the CMPO molecule itself forms polymeric metal complexes the size of which decreases if an excess of ligand is added.[30] The best calculated relaxivity curve of Gd^{3+}·**3** was obtained with the following parameters: $\tau_r = 649$ ps, $\tau_{s0} = 220$ ps, $\tau_v = 29$ ps, and $D = 0.033$ cm^{-1}. All these parameters should be accepted with some reservation because they result from best-fit treatments. Moreover, the rotational time τ_r of Gd^{3+}·**3** should be taken as an approximate minimum value because its actual value has only a limited influence on the shape of the NMRD curves of slowly tumbling complexes. Finally, it should also be noted that no interpretation was possible if a splitting term D was not taken into account when fitting the NMRD data,[25] and it thus seems that the splitting of the zero-field S manifold had to be taken into account under the present experimental conditions. Despite these uncertainties, the NMRD studies clearly indicate that the solution behavior of the lanthanide chelates depends directly on the location of the substituents on the calix unit.

NMRD is of course not the only investigation technique giving access to an analysis of the oligomerization of metal complexes. Among other techniques, NMR spectroscopy of diamagnetic complexes also allows an estimation of the τ_r correlation time. Indeed, τ_r can be deduced from the dipolar part[31] of the ^{13}C spin−lattice relaxation rate $1/T_1^{DD}$

$$\frac{1}{T_1^{DD}} = \frac{nOe}{1.988}\frac{1}{T_1^{exp}} \tag{5}$$

using the equation

$$\tau_r = \frac{1/T_1^{DD} r_{CH}^6}{n_H \gamma_C^2 \gamma_H^2 \hbar^2} \tag{6}$$

where the experimental Overhauser effect (nOe) is compared to the maximum nOe enhancement in eq 6 and where n_H is the number of proton nuclei bonded to a carbon atom at a distance r_{CH}.

The measurement of the experimental nOe and the T_1 relaxation time of the CH groups in the calix unit of La^{3+}·**1** yielded a τ_r value of 120 ps in relatively good agreement with the NMRD studies especially if one takes into account the strong dependence of τ_r upon the actual value of the unknown r_{CH} distance. Negligible Overhauser effects were found in the case of La^{3+}·**3**, in keeping with the high molecular weights of the oligomers formed by this compound. The extreme narrowing condition no longer holds, and eqs 6 and 7 are no longer valid.[31]

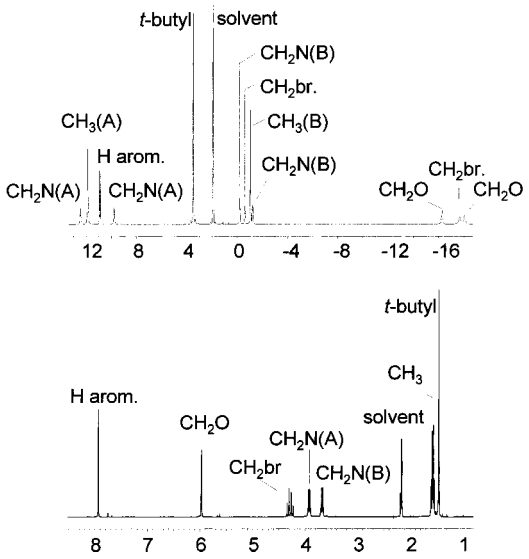

Figure 3. ^1H NMR spectra of the Th^{4+} (bottom) and Yb^{3+} (top, ligand/metal concentration ratio = 1.0) perchlorate complexes with ligand **1** in dry acetonitrile.

Most probably, the unexpected oligomerization of the lanthanide complexes with calixarenes **3**−**8** is not a simple process. A large number of oligomers of different sizes probably coexist in anhydrous acetonitrile. It should also be remembered here that the tumbling time τ_r characterizes the reorientation movements in the immediate vicinity of the Gd^{3+} ions and not of the entire complex.[5] Because a relaxivity maximum is observed in the titration curve of **3** for nearly stoichiometric metal/ligand solutions, one could postulate that under these conditions the oligomers contain approximately one ligand per metal ion. Surprisingly, oligomerization starts to take place in Figure 1 when the ligand/metal ratios are low. Polymeric arrays containing more metal ions than ligands are thus conceivable.

NMR Spectra of the Complexes with Calix[4]arene 1 Substituted at the Narrow Rim. The assignment of the NMR peaks of ligand **1** and of its diamagnetic complexes with La^{3+} and Th^{4+} is easily made from their relative peak areas and splitting patterns. As shown in Figure 3 (bottom), the aromatic protons of Th^{4+}·**1** give rise to a singlet, the O−CH_2−C(O) protons also appear as a singlet, and a pair of doublets (AB pattern) is observed for the methylene protons of the bridges between the aromatic groups. Finally, the two ethyl groups give rise to separate peaks as expected for amide functions. These spectra are consistent with a 4-fold symmetry with the bridging methylene groups featuring protons either in the axial or in the equatorial position relative to the calix unit, as already noted for similar calix[4]arene ligands.[2] Moreover, a rapid inversion of the O−CH_2−C(O) coordinating groups appears to take place, since a single peak is observed for the methylene protons.

Interpreting the spectrum of the Yb^{3+}·**1** complex is less straightforward because the metal ion is paramagnetic. No crystallographic structures of lanthanide or actinide complexes with ligand **1** are available, and the geometry of Yb^{3+}·**1** was calculated by a molecular mechanics force field approach

(29) Cherfa, S. Ph.D. Thesis, University of Paris, 1998.
(30) Diamond, H.; Thiyagarajan, P.; Horwitz, E. P. *Solvent Extr. Ion Exch.* **1990**, *8*, 503−513.
(31) Neuhaus, D.; Williamson, M. P. *The nuclear overhauser effect in structural and conformational analysis*; VCH: Weinheim, 1989.

reported by Hay[17] and Cundari et al.[16] with the parameters supplied by these authors. A near-exact square antiprismatic arrangement of the coordination sphere of Yb^{3+} was found with ligand **1** adopting an arrangement very close to a C_4 symmetry (angle between the diagonals of upper and lower faces = 41.3 ± 0.6°; Figure S3 in the Supporting Information). The NMR spectra of the metal chelates of **1** are in keeping with this structure. Yb^{3+}·**1** displays 13 peaks that are too broad to show any coupling pattern and that are shifted over a 35 ppm range (Figure 3, top). The assignments of these peaks was performed as reported in the Supporting Information after recording the EXSY and correlation spectroscopy (COSY) spectra (Figure S4 and S5) and is shown in Figure 3. The two close resonances assigned to the aromatic units in Figure 3 confirm that the complex adopts a C_4 rather than a C_{4v} conformation as expected for a quasi square-antiprismatic arrangement of ligand **1**. Furthermore, exchange cross-peaks between the proton nuclei in the O−CH_2−C(O) functions provide additional evidence that these functions are involved in inversion of configuration around the encapsulated metal ion. It should be noted here that only a limited number of EXSY and COSY spectra of Yb^{3+} complexes have been reported in the literature essentially because of the very short relaxations times of these paramagnetic species. However, several recently published studies show that 2D spectra of Yb^{3+} chelates can be obtained for complexes of sterically demanding ligands.[5,7] The 2D spectra of Yb^{3+}·**3** are even more illustrative in this respect (vide infra).

It is well-known that the Yb^{3+} ion induces paramagnetic shifts that are essentially dipolar in origin.[5] In cases of axial symmetry (C_3 or above), the induced shift δ_i for each proton i depends only on a simple geometric factor,

$$\delta_i = -D\left\langle \frac{3\cos^2\theta_i - 1}{r_i^3} \right\rangle \qquad (7)$$

where D is a magnetic susceptibility term identical for all nuclei in the complex and where θ_i and r_i are the polar coordinates of proton i in the set of axes of the magnetic susceptibility tensor, the z axis being aligned with the main symmetry axis. Geometric factors were deduced from the structure calculated by molecular mechanics and were compared with the induced paramagnetic shifts. A good linear relationship (Figure S6) was obtained on the basis of eq 7 with an agreement factor[7e] $R = 10.4\%$. This factor becomes larger if the coordinating atoms of ligand **1** are forced to adopt geometries between a cube and a square antiprism as reported for the Pb^{2+}·**1** complex.[32]

NMR Spectra of the Complexes with Calix[4]arenes 3−8 Substituted at the Wide Rim. Well-resolved NMR spectra of mixtures of Th^{4+}, La^{3+}, or Yb^{3+} with **3** were only obtained if a 20−50% excess of metal was added (Figures 4, 5, and S8−S10). Under these conditions, the excess of metal ions has a negligible influence on the relative magnitudes of the dia- and paramagnetic shifts. Broad and poorly shifted peaks were observed under all other conditions including for 1:1 metal/ligand ratios.

The NMR spectrum of Th^{4+}·**3** is shown in Figure 4. Complete assignment of this spectrum is straightforward based on the relative areas of the peaks, their J couplings, and the COSY (Figure S7) and ROESY spectra. Two features are particularly noteworthy: the aromatic groups give rise to two peaks (6.60 and 7.41 ppm) that are coupled with each other (J = 3.08 Hz in a J resolved spectrum) and the bridging CH_2 protons in the calix unit appear as two AX forms ($CH_{2\ br}$ in Figure 4). It thus appears that the calix moiety of ligand **3** adopts a 2-fold symmetry rather than the C_4 geometry proposed for the chelates with calixarene **1**. Because of this lower symmetry, the protons of the α-CH_2 groups in the propylene chains of **3** are diastereotopic and appear as a doublet of multiplets around 4 ppm. Rapid exchange between two conformations of the NH−CH_2−P(O) groups is indicated by the presence in the spectrum of but a single resonance peak for the NH protons and the ^{31}P nuclei at 9.96 and 46.9 ppm, respectively.

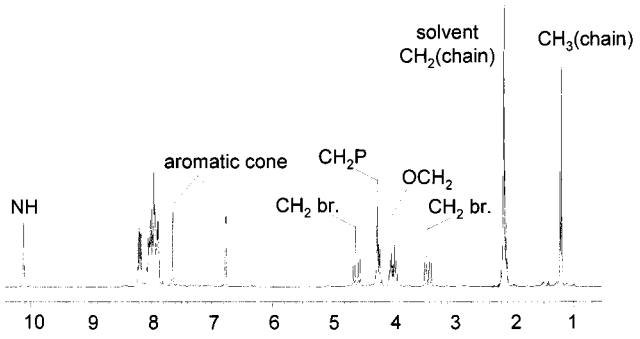

Figure 4. ^1H NMR spectrum of the Th^{4+} perchlorate complex with ligand **3** in dry acetonitrile (ligand/metal concentration ratio = 0.65).

The NMR spectra of La^{3+}·**3** and Th^{4+}·**3** are similar and display the same C_2 symmetry (Figures S8 and 4). The spectrum of Yb^{3+}·**3** in the presence of an excess of metal ions covers a 60 ppm range at 298 K. On the other hand, a 1:1 solution of Yb^{3+} and **3** gives rise to broad, poorly shifted peaks, but bringing the temperature down to 260 K allowed one to observe NMR peaks associated with at least two species: a major component that exhibits strongly overlapping peaks between 0 and 12 ppm and a minor component that features poorly resolved peaks covering a 80 ppm range. The number of peaks assigned to this latter species and their relative positions are in qualitative agreement with the spectra obtained in the presence of an excess of metal and reported in Figures 5 and S9−S10. This behavior is ascribed to a fast exchange between several polymeric derivatives and a monomeric rigid species. The spectroscopic studies are limited to solutions containing an excess of Yb^{3+}, and it will thus be assumed that one species, presumably a 1:1 complex, largely predominates in solution and is exchanging rapidly on the NMR time scale with oligomeric derivatives and possibly with a 2:1 metal/ligand complex. The predominance of a 2:1 complex is unlikely despite an excess of metal ions because this species would be less stable and more labile than the 1:1 species and could not give rise to the highly resolved spectra shown in Figure 5. Indeed, highly resolved NMR spectra of Yb^{3+} chelates have so far been obtained only for highly rigid species as indicated in ref 7. A complex between **3** and two $La(NO_3)_3$ units has been isolated and characterized,[29] but each metal is directly coordinated to three nitrate ions that are known to be much better able to complete the coordination sphere of lanthanides than the perchlorate ions used in the present work. Finally, it should be noted that NMRD curves featuring a relaxivity maximum as in Figure 2 are easily simulated by assuming that only a small part of the ligand (10% or less) forms oligomeric species in the presence of an excess of metal ions. Observing an oligomerization in the NMRD curves and obtaining highly resolved NMR spectra under the same conditions of concentrations is thus not contradictory.

A quantitative analysis of the NMR spectra of Yb^{3+}·**3** will obviously be thwarted by the oligomerization processes, as

(32) Beer, P. D.; Drew, M. G. B.; Leeson, P. B.; Ogden, M. I. *J. Chem. Soc., Dalton Trans.* **1995**, 1273−1283.

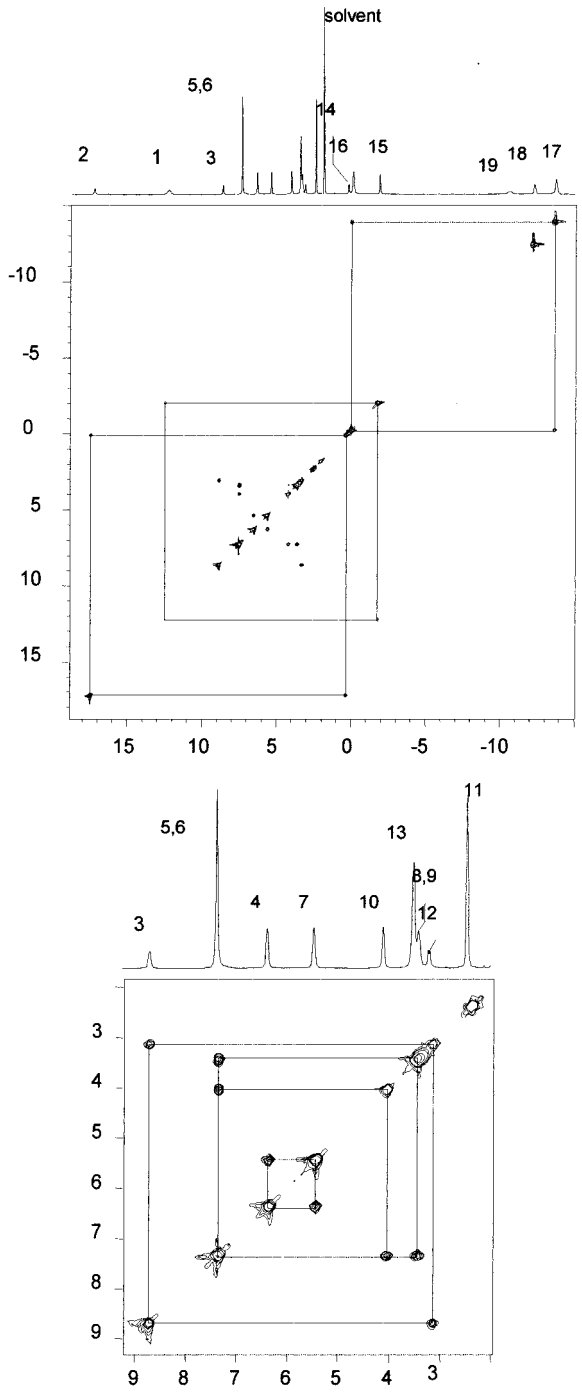

Figure 5. EXSY spectrum of the Yb^{3+} perchlorate complex with ligand **3** in dry acetonitrile at 345 K (ligand/metal concentration ratio 0.59) with the following peak assignments: calix phenyl H, 1, 15; calix bridging C*H*$_2$, 2, 3, 12, 14; C(O)C*H*$_2$−P(O), 18, 19; P−phenyl H, 5, 10 (para), 6, 13 (ortho), 10, 16 (meta).

evidenced by the NMRD studies. One should not expect to reach a quantitative agreement between the experimental and calculated paramagnetic shifts as in the case of ligand **1**. The Yb^{3+}·**3** complex in anhydrous acetonitrile features 19 NMR peaks covering a 30 to −40 ppm range with 4 peaks of unit area, 10 peaks of area 2, 4 peaks of area 4, and 1 peak of area 6. A total of 46 relative area units is obtained for 92 protons in ligand **3**, the amide protons not being taken into account as they give rise to one or more large peaks that are difficult to distinguish from the background noise even at the lowest temperatures. A C_2 symmetry is thus assigned to Yb^{3+}·**3**. The relative areas of the NMR peaks, the *J* coupling cross-peaks and the exchange

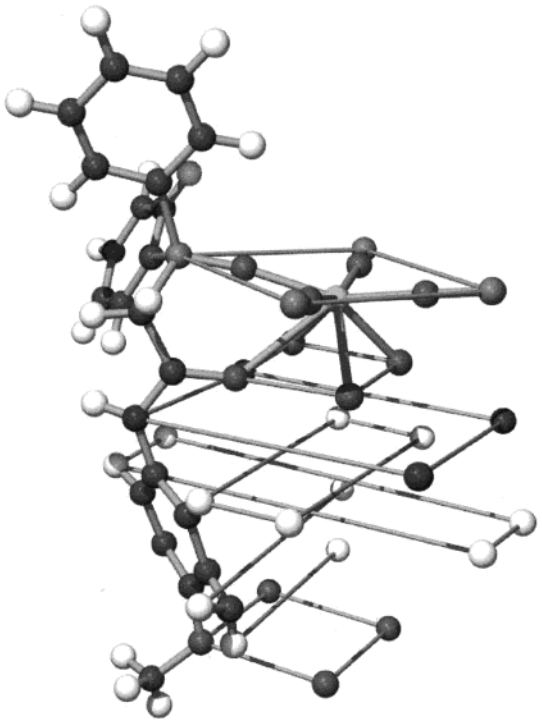

Figure 6. Schematic representation of the structure suggested for the 1:1 Yb^{3+}·**3** complex. From bottom to top are the phenolic O_4 plane, two lines joining protons in equivalent bridging methylene groups, two planes of aromatic protons, and N_4, O_4, and P_4 planes. The *x* and *y* axes of the susceptibility tensor must be perpendicular to the sides of the rectangles and squares formed by the different groups of atoms.

cross-peaks displayed in the COSY and EXSY spectra of Yb^{3+}·**3**, are listed in Table S1 in the Supporting Information together with the peak assignments that are also given in the legend of Figure 5. The reasoning followed to analyze these spectra is reported in the Supporting Information. To take into account all the spectral features displayed by Yb^{3+}·**3**, the structure of this complex should be built in such a way that a geometry of 2-fold symmetry is obtained with (a) a calix cone in which the aromatic rings are linked together by methylene groups in two different environments in which each type of methylene must feature two nonequivalent protons, (b) a calix cone with two groups of four equivalent aromatic protons, (c) four equivalent −P−CH_2−CO− moieties containing two nonequivalent protons, (d) two types of phenyl rings on the phosphine oxide moieties, (e) four equivalent phosphine oxide functions, (f) four equivalent propylene substituents on the narrow rim.

Several hypotheses can be put forward to account for the 2-fold symmetry of Yb^{3+}·**3**. A square arrangement of the phosphine oxide groups in a planar array is expected,[33] but other possibilities cannot be excluded. For instance, a rectangular arrangement of *P*(O) functions or the sharing of these functions between several metal ions in a stable oligomeric structure would also lead to a 2-fold symmetry. These geometries are not favored firstly because of steric reasons and secondly because the drastic effect of an excess of metal ions on the NMR spectra seems to indicate that a single 1:1 complex predominates in solution. Figure 6 shows a model that takes into account the geometrical requirements deduced from the NMR spectra as listed above. This structure was built as reported in the experimental part, and it is assumed that the 2-fold symmetry arises from an

(33) Kepert, D. L. *Inorganic stereochemistry*; Springer-Verlag: Berlin, 1982; pp 1−227.

Chart 2

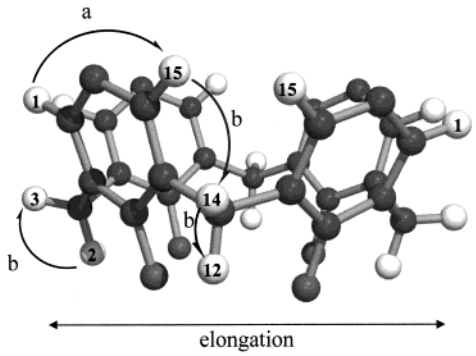

a: EXSY, b: COSY

elongation of the calix unit as illustrated in Chart 2. Models indicate that a square antiprismatic coordination geometry could force the calixarene moiety to adopt such an elongated conformation. For the sake of clarity, only part of the complex is shown in Figure 6 but the members of each group of equivalent donor atoms or equivalent protons are linked together. The coordination sphere of the metal ion is a square antiprismatic arrangement of oxygen atoms. The structure is made up of parallel rectangles or squares that are successively, from bottom to top, an O_4 plane for the phenol oxygens (square), two planes for the two types of aromatic protons in the cone unit (rectangles), and finally, planes of amide nitrogens, amide oxygens, and phosphorus atoms (squares). In addition, the two members of each of the four groups of bridging methylene protons can be linked by lines that are parallel to the planes presented in Figure 6 and are medians of all these geometric forms (only two such lines are shown). Similarly, the protons of the phenyl substituents on the phosphine oxide groups also form parallel square figures (not shown). This structure fully accounts for the number of NMR peaks of Yb^{3+}·**3** and for their relative areas. Unrealistic bond angles and bond distances were obtained if the sides of the square formed by the phosphorus atoms were forced to be parallel to the sides of the rectangles formed by the protons in the calix unit, that is, if the coordination sphere of the metal ion is prismatic rather than square antiprismatic.

The full dipolar eq 8 must be used to correlate the relative magnitudes of the induced paramagnetic shifts of Yb^{3+}·**3** with the proposed geometry, since this complex is not axially symmetric,

$$\delta_i = -D\left\langle \frac{3\cos^2\theta_i - 1}{r_i^3} \right\rangle - D'\left\langle \frac{\sin^2\theta_i \cos 2\varphi_i}{r_i^3} \right\rangle \qquad (8)$$

where D and D' are magnetic susceptibility parameters and where r_i, θ_i, and φ_i are the polar coordinates of nucleus i as defined for eq 7. Applying this equation requires that the x and y axes are properly oriented while the z axis coincides with the C_2 axis of symmetry. This equation has already been used successfully for a quantitative analysis of the solution structure of several Yb^{3+} complexes[6,34,35] of low symmetry. In these studies, best-fit treatments yielded reasonable orientations of the x and y axes, for instance, in two perpendicular planes bisecting the donor atoms of the ligands in a rigid conformation. Equation 8 leads at best to a semiquantitative agreement between the calculated and the experimental paramagnetic shifts for Yb^{3+}·**3**. Restricting the calculations to the protons of the calix unit does not bring any improvement despite the rigidity of this structure nor does a variation of its elongation between 6 and 8 Å. Taking into account all the protons in the structure presented in Figure 6 leads to an agreement factor $R = 46\%$ for the low-temperature spectra of Yb^{3+}·**3** while much lower values such as $R = 8.9\%$ have been reported for other complexes of 2-fold symmetry.[34] A poor agreement between the expected structure and the $1/T_1$ relaxation rates of all protons of Yb^{3+}·**3** was also found despite the expected dependence[5] of this factor with r_i^{-6}. These difficulties are not surprising in view of the unusual solution behavior of ligand **3**, and it is much more difficult to unravel with certainty the solution structure of calixarene complexes bearing substituents on their wide rim. However, the good resolution of the spectra reported in Figures 5 and S8−S10 points to the predominance of one single species in solution for which the peak assignment is valid as well as the overall geometry ascribed to Yb^{3+}·**3** in Figure 6.

The cross-peak patterns in the EXSY spectra yield interesting information on the exchange processes taking place in the Yb^{3+}·**3** complex. As shown in Table S1, exchange cross-peaks are found between the different aromatic and methylenic protons in the calix unit. It thus appears that the cone structure with 2-fold symmetry undergoes a breathing movement in which the two bridging methylene groups that are located along the line of elongation are moving closer to each other while the two other bridging groups are moving apart (see Chart 2). In this process, the direction of elongation becomes perpendicular to its original orientation and the bridging methylenes exchange their positions as do the phenyl protons. In addition, a rotation process takes place in the coordination sphere of the Yb^{3+} ion, since exchange cross-peaks are observed between the two types of phenyl−P═O groups. The activation parameters for the movement of the calix unit were measured by integrating the diagonal and cross-peaks for the exchange between the phenyl protons in the EXSY spectra of the diamagnetic complex La^{3+}·**3** at different temperatures. A linear Eyring plot (Figure S11) was obtained for La^{3+}·**3** with $\Delta H^{\ddagger} = 69.3 \pm 7.2$ kJ mol^{-1}, $\Delta S^{\ddagger} = -27 \pm 22$ J K^{-1} mol^{-1}.

The NMR spectra of the complexes formed by ligands **5** and **8** were also analyzed (Figures S12 and S13). The 1D and 2D NMR spectra of Yb^{3+}·**5** are closely related to the corresponding spectra obtained with ligand **3** under the same experimental conditions, taking into account the different substituents on the phosphine oxide and phosphonate functions. The number of peaks and their relative areas are in keeping with the overall geometry proposed for the derivatives of ligand **3**. Moreover, the dipolar eq 8 again leads to no more than a semiquantitative agreement with the calculated structure. Free ligand **8** exhibit very complicated ^{1}H and ^{31}P NMR spectra presumably because it can adopt several arrangements in solution because its methyl substituents are not bulky enough to preclude the formation of "partial cone" or "1,3-alternate" conformations.[3] Adding a lanthanide ion immediately leads to spectra that can be assigned to one single conformation of the regular "cone" type as illustrated in Chart 2. The dissymmetry of the ligand due to its different substituents has no effect on the number of peaks assigned to the calix unit but the ^{1}H peaks assigned to the C(O)−CH_2−P(O) and the phenyl−P(O) groups are split in two. A single ^{31}P at 40.5 ppm is found in the spectrum of La^{3+}·**8**, but Yb^{3+}·**8** exhibits two ^{31}P NMR peaks at −71.5 and −74.6 ppm

(34) Desreux, J. F.; Loncin, M. F. *Inorg. Chem.* **1986**, *25*, 69−74.
(35) Forsberg, J. H.; Delaney, R. M.; Zhao, Q.; Harakas, G.; Chandran, R. *Inorg. Chem.* **1995**, *34*, 3705−3715.

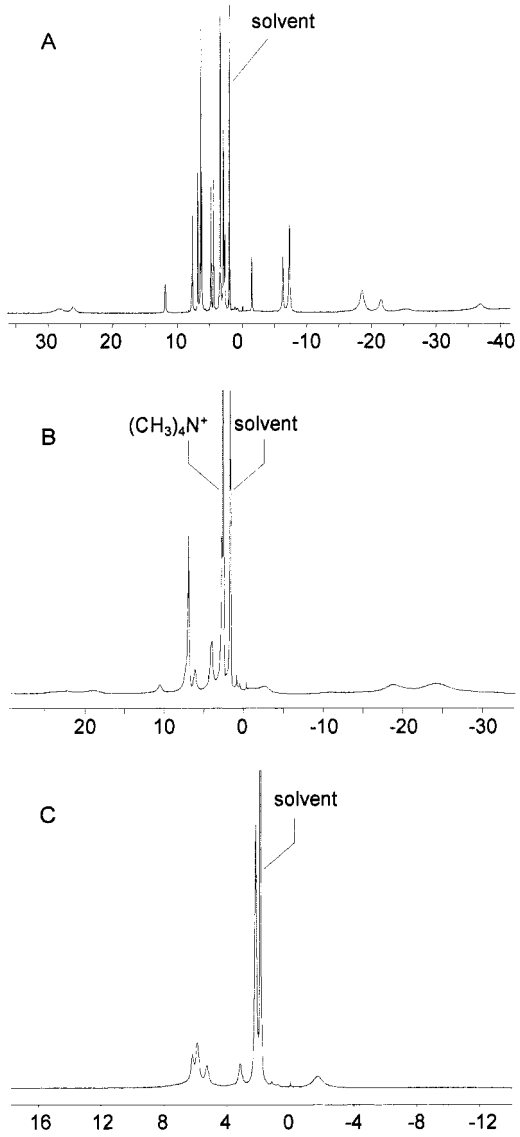

Figure 7. ^{1}H NMR spectrum of the Yb^{3+}·**3** complex in acetonitrile at 298 K (A) and effect of the addition of 1−2 equiv of tetramethylammonium nitrate (B) and of water (C).

at 298 K. Because of the difficulties already encountered with ligand **3**, no quantitative analysis of the NMR spectra was carried out.

Effect of Anions and of Water. The above NMR studies were performed under anhydrous conditions and with metal salts of the very poorly coordinating perchlorate anion. Solvent extraction processes are carried out in the presence of aqueous phases containing much more strongly complexing anions such as NO_3^- or Cl^-. It was thus interesting to investigate the effect of water and of nitrate ions on the solution structure of the complexes of calixarenes **1** and **3**. The addition of an excess of tetramethylammonium nitrate or of water has no effect on the NMR spectrum of Yb^{3+}·**1** (Figure S13) but drastically alters the spectrum of the corresponding complex with ligand **3** (Figure 7). In the latter case, all resolution is lost and only broad and poorly shifted NMR peaks are observed. In keeping with the relaxation data presented in Figures 1 and 2, calixarene **1** forms stable lanthanide complexes with a rigid coordination sphere that does not allow the replacement of its donor groups by water or nitrate ions. By contrast, the geometry of the complexes with ligand **3** is very easily labilized and it is likely that numerous species of different structures coexist in solution and are in fast exchange on the NMR time scale when water and/or nitrate ions are present.

Conclusion

Substituting a calix[4]arene unit at the narrow or at the wide rim has a dramatic effect on the complexation properties of the resulting ligands toward the lanthanides and Th^{4+}. Oxygen-containing coordinating groups at the narrow rim form a rigid cage, and highly symmetric metal complexes are obtained, the structure of which is not altered by the addition of water or of nitrate ions and can be interpreted by the NMR dipolar equations in the case of Yb^{3+}. NMRD analyses clearly show that these complexes are monomeric in anhydrous acetonitrile. By contrast, carbamoylmethyl phosphine oxide groups substituting the more open wide rim of a calix[4]arene are flexible and appear to be involved in the formation of polymeric species. Moreover, water and nitrate ions easily compete with the donor groups of the ligand and labilize the Yb^{3+} complex. When used as extracting agents of the lanthanides, the very high selectivity[4] of ligands such as **3** thus stems from a intricate interplay of factors that can be partially assessed by NMR spectroscopy.

Finally, the present investigation demonstrates that the utility of relaxivity measurements is not limited to aqueous solutions. Measurements in acetonitrile at different frequencies and different metal/ligand concentration ratios afford conclusive evidence of the formation of oligomers.

Acknowledgment. This work has been financially supported by the European Commission in the framework of the research program on "Management and Storage of Radioactive Waste". The Liege research group gratefully acknowledges the financial support of the Fonds National de la Recherche Scientifique and the Institut Interuniversitaire des Sciences Nucléaires. B.L. is Aspirant at the IISN and V.J. is Chercheur Qualifié at the FNRS. The authors are grateful to Prof. R. N. Muller, University of Mons-Hainaut, Belgium, for NMRD measurements and to Prof. C. Luchinat, University of Florence, Italy, for helpful discussions.

Supporting Information Available: Listing of procedure followed for the assignment of the NMR peaks of Yb^{3+}·**1** and Yb^{3+}·**3** (Table S1) with coupling patterns in the COSY and EXSY spectra of Yb^{3+}·**3**, figures with the relaxivity titration of Gd^{3+} by **7** (Figure S2), optimized structure of Gd^{3+}·**1** (Figure S3), COSY and EXSY spectra of the Yb^{3+}·**1** (Figures S4 and S5), correlation between experimental and calculated induced paramagnetic shifts of Yb^{3+}·**1** and Yb^{3+}**3** (Figure S6), COSY spectrum of Th^{4+}·**3** (Figure S7), ^{1}H NMR spectrum of La^{3+}·**3** (Figure S8), ^{1}H NMR spectrum of Yb^{3+}·**3** (Figure S9), COSY spectrum of the Yb^{3+}·**3** chelate at 273 K in dry acetonitrile (Figure S10), Eyring plot for La^{3+}·**3** (Figure S11), ^{1}H NMR spectra of Yb^{3+}·**5** (R_2 = propyl) (Figure S12) and of Yb^{3+}·**8** (Figure S13), ^{1}H NMR of Yb^{3+}·**1** after addition of water or tetramethylammonium nitrate (Figure S14). This material is available free of charge via the Internet at http://pubs.acs.org.

IC990683N